Ferromagnetic hcp Chromium in Cr/Ru(0001) Superlattices

M. Albrecht,[1,*] M. Maret,[1,2] J. Köhler,[1] B. Gilles,[3] R. Poinsot,[2] J. L. Hazemann,[4] J. M. Tonnerre,[4] C. Teodorescu,[5] and E. Bucher[1]

[1]*Department of Physics, University of Konstanz, D-78457 Konstanz, Germany*
[2]*IPCMS, CNRS-ULP, 23 rue du Loess, F-67037 Strasbourg, France*
[3]*LTPCM-ENSEEG, F-38402 Saint-Martin d'Heres, France*
[4]*Laboratoire de Cristallographie, CNRS, F-38042 Grenoble, France*
[5]*LURE, F-91898 Orsay, France*

(Received 11 August 2000)

We report the first observation of a weak ferromagnetic state of Cr in Cr/Ru(0001) superlattices, based on magnetic hysteresis and corroborated by x-ray magnetic circular dichroism at the Cr $L_{2,3}$ edges. *In situ* reflection high-energy electron diffraction, x-ray diffraction, and Cr *K*-edge polarized x-ray absorption investigations have shown that the Cr layers thinner than 8 Å adopt a slightly distorted hcp structure, accompanied by a large atomic volume expansion of up to 14% compared to the bcc packing volume. The expanded hcp structure clearly induces the observed ferromagnetism, in agreement with theory.

PACS numbers: 61.10.Ht, 61.14.Hg, 68.60.–p, 75.70.–i

The difference in physical properties of ultrathin films compared to bulk materials has been the key motivation for extensive research devoted to the growth of metal films. These changes are due to either the reduced dimensions or a crystalline structure different from the equilibrium state; the latter may arise when the lattice constants or crystal symmetries of film and substrate are different. Especially, the magnetic properties are predicted to change drastically upon changing the crystal structure or interatomic distances. Cr is a 3*d* transition metal showing antiferromagnetism [1] with a small magnetic moment ($\approx 0.6\mu_B$) in its condensed bcc form and a very large moment ($\approx 5\mu_B$) in its atomic form suggesting that peculiar magnetic effects might be observed in ultrathin Cr layers. The Stoner theory of ferromagnetism has been applied to 3*d* transition metals in the hexagonal close packed (hcp) phase and Cr was proposed to be ferromagnetic [2]. Another theoretical approach based on self-consistent linear muffin-tin orbital calculations also predicts a stable but weak ferromagnetic ground state for hcp Cr with a magnetic moment of $0.1\mu_B$ per Cr atom [3]. In this Letter we report the stabilization of Cr layers with an expanded hexagonal structure by pseudomorphic molecular beam epitaxy (MBE) growth on a metal surface exhibiting hcp symmetry. Several groups attempted to prepare metastable chromium on different metal substrates like Au(100) [4,5], Cu(001) [6–8], Ag(100) [9], Pt(111) [10], and Co(0001) [11], but scarce information about the magnetic properties was presented. In contrast, a successful stabilization of hcp Fe on Ru(0001) was clearly reported [12]. Because of the similar bcc Fe and Cr lattice parameters, we tried to grow hexagonal Cr on Ru(0001).

The multilayered films were prepared in a MBE chamber and the growth was analyzed by *in situ* reflection high-energy electron diffraction (RHEED). The pressure in the MBE chamber did not exceed 5×10^{-8} Pa during metal deposition. First, a 50-Å-thick Ru buffer layer was deposited at 923 K on a $SrTiO_3(111)$ substrate with a deposition rate of 0.1 Å/s. Then, Cr and Ru layers were alternately grown at room temperature with a deposition rate of 0.1 Å/s. The compositions of the studied multilayers are $SrTiO_3(111)$/Ru(50 Å)/$[Cr(t)/Ru(10\ Å)]_{20}$/Ru(10 Å), where the Cr layer thickness *t* ranges from 4 up to 20 Å. All samples were covered with an additional 10-Å-thick Ru layer to prevent the samples from oxidation. Details of the sample preparation and growth conditions have been previously reported [13,14]. After the deposition of several Cr/Ru bilayers, the surface becomes rougher and the RHEED patterns are dominated by transmission electron diffraction directly bringing information on the type of stacking sequence. Figure 1 shows the RHEED patterns, recorded along the $[11\bar{2}0]$ direction referred to Ru(0001), after the tenth layer of 10 Å Ru in the multilayer growth sequence and after

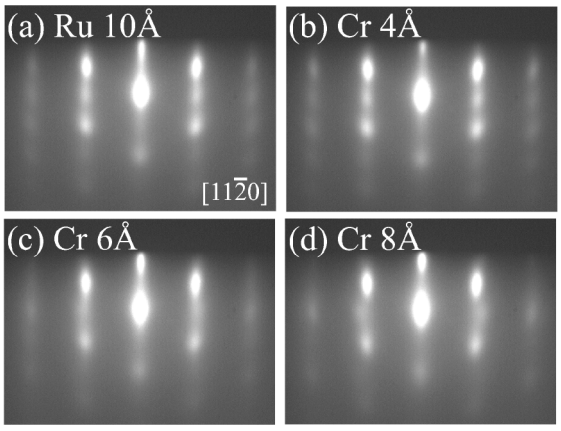

FIG. 1. RHEED patterns along the $[11\bar{2}0]$ azimuth taken during the growth of a $[Cr(10\ Å)/Ru(10\ Å)]_{20}$ multilayer: (a) after the tenth layer of 10 Å Ru; (b),(c),(d) after the deposition of 4, 6, and 8 Å Cr, respectively.

 0031-9007/00/85(25)/5344(4)$15.00

the deposition of the following Cr layer. The 3D RHEED pattern of Ru [Fig. 1(a)] is characteristic for a hcp stacking sequence with two intense spots separated by a weaker spot along the two streaks on both sides of the central streak. After the growth of 4 Å of Cr, this pattern is not modified, after 6 Å the intermediate spots along the two streaks disappear, and from 8 Å a middle spot appears again but is shifted, indicating a smaller in-plane distance. In Fig. 1(d) the relaxation process is almost finished and the pattern reveals clearly the superposition of three bcc(110) domains, one with the [110] direction parallel to Ru[$1\bar{1}00$] and two other bcc(110) domains rotated from $\pm 60°$, following the Nishiyama-Wassermann epitaxy mode [15].

During the deposition of Cr on Ru, the recording of line scans extracted from the RHEED patterns allows us to follow the in-plane lattice parameter along the [$11\bar{2}0$] and [$1\bar{1}00$] azimuths and gives us the possibility to measure the anisotropic lattice relaxation of Cr on the surface. In the case where Cr relaxes completely in its bcc structure along the [$1\bar{1}00$] direction the lattice parameter should change from $a_{\mathrm{Ru}}^{\mathrm{hcp}}\sqrt{3}$ to $a_{\mathrm{Cr}}^{\mathrm{bcc}}\sqrt{2}$, and along the [$11\bar{2}0$] direction from $a_{\mathrm{Ru}}^{\mathrm{hcp}}$ to $a_{\mathrm{Cr}}^{\mathrm{bcc}}$. Starting from the perfect hcp Ru surface the ratio of these two distances of $\sqrt{3}$ decreases with the Cr deposited thickness almost towards the ideal bcc value of $\sqrt{2}$ after 20 Å, with a pronounced decrease between 6 and 8 Å. In contrast, the growth of Ru on Cr shows an immediate relaxation towards the hcp(0001) structure finished after only 1–2 monolayers (ML). From our RHEED observations, it turns out that up to 6 Å (≈3 ML) Cr grows pseudomorphically on Ru(0001) and above relaxes into the bcc structure. However by covering again by a Ru layer, an increase of the Cr thickness constrained in the hcp structure can be expected in the buried layers.

In order to elucidate this point and to confirm the hexagonal structure of the thin Cr layers, we have used x-ray diffraction (XRD), polarized x-ray absorption fine structure (XAFS), and x-ray absorption near-edge structure (XANES) spectroscopy. The XRD measurements were performed at the European Synchrotron Radiation Facility (ESRF) on the CRG BM02 beam line in Grenoble (France) using a wavelength of 1.5517 Å. Figure 2 shows a XRD θ-2θ scan of a superlattice with $t = 6$ Å. Besides the 111 $SrTiO_3$ peak and the two series of Kiessig fringes arising from the Ru buffer and total superlattice thicknesses, satellite peaks around the mean 0002 superlattice (SL) Bragg peak are clearly observable for all superlattices.

The spacing of planes along the growth direction in the Cr layers, d_{Cr}, was determined by simulating the diffraction pattern with the software program SUPREX [16], assuming a spacing of Ru(0002) planes equal to that of a bulk one (2.14 Å). For Cr layers smaller than 8 Å, d_{Cr} is close to that of Ru(0002) and the normal coherence length $L_\perp$, deduced from the width (FWHM) of the 0002 SL peak, is in the range of the total superlattice thickness. From 8 Å, $L_\perp$ decreases rapidly and d_{Cr} approaches the spacing of the (110) planes in bcc Cr equal to 2.04 Å. In order to summarize the structural XRD and RHEED data, the atomic volume of Cr, V_{Cr}, as a function of the Cr layer thickness is displayed in Fig. 3. For the superlattices with $t = 4$ and 6 Å we found an increase of the Cr atomic volume of about 14% compared to the bulk phase and between 6 and 8 Å a pronounced relaxation due to a structural change of the Cr layers.

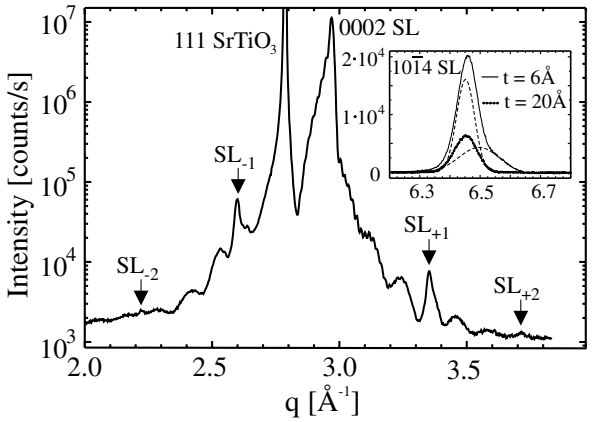

FIG. 2. X-ray intensity (θ-2θ scan) around the 0002 Bragg peak of a Cr/Ru superlattice with $t = 6$ Å, $q = 4\pi \sin\theta/\lambda$. The inset shows the intensities around the 10$\bar{1}$4 reflection for two superlattices with $t = 6$ and 20 Å.

XRD measurements were also performed in asymmetric reflection geometry, which allows the separation between reflections characteristic of the bcc and hcp structures. For the superlattice with $t = 20$ Å we have measured a broad bcc 130 peak, found exactly at the position expected for bulk bcc Cr ($q = 6.9$ Å^{-1}) (see inset in Fig. 2). The width of this peak leads to a coherence length $L_\perp$ restricted to the thickness of a single Cr layer, indicating the absence of coherent diffraction between two successive Cr layers. For the superlattice with $t = 6$ Å no bcc 130 reflection was

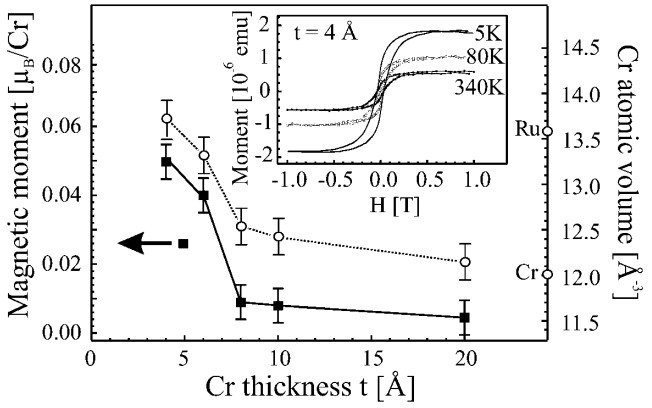

FIG. 3. Cr atomic volume (open circles) and magnetic moment per Cr atom (solid squares) as a function of the Cr layer thickness t. The bulk values for bcc Cr and hcp Ru are also indicated on the right axis. The inset shows temperature-dependent hysteresis loops for a Cr/Ru superlattice with $t = 4$ Å.

observed. In contrast, a strong increase of the hcp $10\bar{1}4$ reflection intensity was measured compared to that found in the superlattice with $t = 20$ Å coming only from the Ru buffer; the $10\bar{1}4$ peak for the sample with $t = 6$ Å can be reproduced by the sum of two Gaussians: one located at the bulk $10\bar{1}4$ Ru position ($q = 6.45$ Å^{-1}) and the other somewhat broader at $q = 6.49$ Å^{-1}. The increase of the $10\bar{1}4$ intensity by decreasing the Cr layer thickness reflects the extent of the normal coherence through several layers, owing to the stabilization of Cr hexagonal where the spacing of Cr(0002) planes is slightly smaller than the one of Ru(0002) planes as indicated by the shift of the broad peak.

XAFS and XANES experiments were carried out on the CRG BM32 beam line at the ESRF for each Cr/Ru multilayer at room temperature. The linear polarization of the x-ray beam renders the technique sensitive to crystallographic anisotropy. Two spectra were collected at the Cr-K edge ($E_0 = 5993$ eV) using a total electron yield detector: one under grazing incidence corresponding to the out-of-plane polarization and the other under normal incidence corresponding to the in-plane polarization. From Fig. 4 it appears that the polarization dependence decreases gradually when t increases and vanishes completely for t equal to 20 Å. As calculated by Brouder [17], the XANES spectra are independent on polarization for cubic symmetry, while for the hexagonal structure they exhibit an anisotropy, already observed in Co thin films [18]. In our case, the well marked polarization dependence found in the superlattices

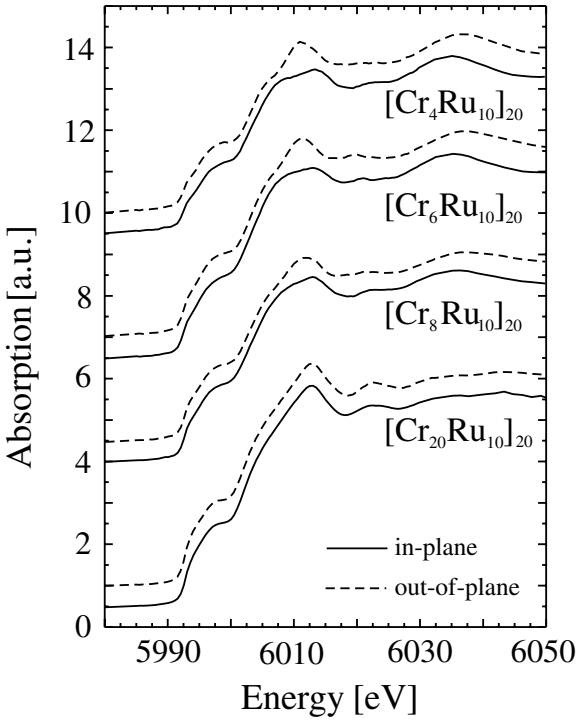

FIG. 4. Cr-K XANES spectra measured for in-plane (solid curves) and out-of-plane (dashed curves) polarization. The curves were shifted for clarity.

for $t = 4$ and 6 Å is again a signature of the hexagonal Cr, while for $t = 20$ Å the two spectra are identical in agreement with a bcc stacking.

The analysis of the XAFS spectra yields the determination of the neighbor distances and the corresponding coordination numbers. Using the standard XAFS formula [19], we present only the analysis of the nearest neighbor filtered XAFS signals for out-of-plane polarization, since only the atoms out of the (0001) hcp or (110) bcc planes contribute to these signals. The separation between the two possible stackings in the Cr layers, hcp and bcc, can be established by simulating the filtered signals by two or three shells, respectively, corresponding to one Ru shell and one or two Cr shells. Indeed, in a perfect hcp stacking of (0001) planes the first neighbor shell is described by one distance with 12 neighbors, and in a perfect bcc stacking of (110) planes by two distances ($\frac{\sqrt{3}}{2}a^{\mathrm{bcc}}$ and a^{bcc}) with eight atoms and six atoms, respectively. In our simulations, the Ru and Cr coordination numbers were fixed, assuming a perfect structure of the superlattices (2 Å $\sim$ 1 ML). They depend on both the structure and thickness of the Cr layers; for example, for $t = 4$ Å the Cr atoms in the two monolayers would have six Ru neighbors and six Cr neighbors for Cr hcp layers or a two-shell Cr distribution (four and three atoms, respectively) for Cr bcc layers. It turns out that for $t = 4$ and 6 Å, two shells (Cr-Cr at 2.5 Å and Cr-Ru at 2.57 Å) are sufficient for reproducing the filtered signals, while from 8 Å the addition of a second Cr-Cr shell around 2.87 Å is necessary. Finally, the XAFS and XANES measurements confirm as well the stabilization of an hexagonal phase in the Cr layers up to 6 Å. The interesting question is how this pronounced structural change of Cr modifies the magnetic properties?

The magnetization measurements were performed at 5 K using a superconducting quantum interference device (SQUID) magnetometer (magnetic field was applied in the film plane). All samples present magnetization hysteresis loops with parallel remanences and coercitivities varying from 35% to 30% and from 400 to 200 Oe, respectively. Indeed, the absence of a magnetization hysteresis loop for a 500-Å-thick Ru buffer layer grown on $SrTiO_3(111)$ at 923 K allows us to exclude the formation of a ferromagnetic alloy at the interface Ru/$SrTiO_3$. Furthermore, the formation of Cr-Ru compounds at the interfaces can be ruled out from RHEED investigations. When the Cr layer thickness increases from 4 to 20 Å, the magnetic moment per Cr atom at 5 K decreases from 0.05 to $0.005\mu_B$. This behavior is displayed in Fig. 3. It is straightforward that the change of the magnetic moment with the Cr thickness follows closely the decrease of the Cr atomic volume. The nonvanishing moment in the thicker Cr layers may be explained by the existence of distorted hcp Cr located at the Ru/Cr interface. In addition, temperature-dependent magnetization measurements up to 340 K for the superlattice with $t = 4$ Å have shown a continuous decrease of the magnetic moment, indicating that the Curie temperature is higher (see inset in Fig. 3).

To confirm that the ferromagnetism can be attributed to hcp Cr layers, we have performed x-ray magnetic circular dichroism (XMCD) measurements on the SU23 beam line of the positron storage ring SuperACO at LURE (Orsay, France). The absorption spectra were monitored at 1.5 K in the total electron yield detection mode at the Cr-$L_{2,3}$ edges. The XMCD signal was obtained by reversing the direction of the applied magnetic field with respect to the direction of the incident beam, keeping the helicity of the photon beam fixed. The incident beam strikes the sample surface under an incidence of 45°. A magnetic field of ± 5 T was applied to saturate the two studied superlattices ($t = 4$ and 6 Å). For both samples we have measured a weak XMCD signal (0.5% of the total Cr absorption signal), characterized by a negative L_3 peak followed by a small positive peak and a positive L_2 peak, similar to that observed by O'Brien and co-workers for a submonolayer of Cr on Fe [20].

Because of the small spin-orbit coupling of the Cr $2p$ states, the application of the spin sum rule [21] should yield an underestimate of the magnetic moment. Nevertheless, from the integrated XMCD signals at the $L_{2,3}$ edges and assuming a number of $3d$ holes equal to 5, we obtained a Cr spin magnetic moment of about $(0.05 \pm 0.02)\mu_B$ for both samples in excellent agreement with the SQUID data.

In summary, the observed ferromagnetism in Cr/Ru superlattices can be firmly correlated with the structural expansion of the Cr layers in an hcp stacking. Thereby, this expansion induces a change from antiferromagnetic to ferromagnetic order in agreement with band-structure calculations. The authors of Ref. [3] pointed out that they believe to have formulated the guidelines for MBE engineers to produce new magnetic materials in hcp phases by MBE. And indeed, we found a particular case where theoretical predictions and experimental realization are in excellent agreement.

This project was supported by the Deutsche Forschungsgemeinschaft (SFB 513), which is gratefully acknowledged.

*Corresponding author.
Email address: manfred.albrecht@uni-konstanz.de

[1] E. Fawcett, Rev. Mod. Phys. **60**, 209 (1988).
[2] D. A. Papaconstantopoulos, J. L. Fry, and N. E. Brener, Phys. Rev. B **39**, 2526 (1989).
[3] M. Podgórny and J. Goniakowski, Phys. Rev. B **42**, 6683 (1990).
[4] M. C. Hanf *et al.,* Phys. Rev. B **39**, 3021 (1989).
[5] C. Rau *et al.,* Phys. Lett. A **135**, 227 (1989).
[6] J. Jandeleit, Y. Gauthier, and M. Wuttig, Surf. Sci. **319**, 287 (1994).
[7] D. Rouyer *et al.,* Surf. Sci. **307–309**, 477 (1994).
[8] D. Rouyer *et al.,* Surf. Sci. **322**, 34 (1995).
[9] D. Rouyer *et al.,* Surf. Sci. **331–333**, 957 (1995).
[10] L. Zhang, M. Kuhn, and U. Diebold, Surf. Sci. **371**, 223 (1997).
[11] P. Ohresser *et al.,* Surf. Sci. **352–354**, 567 (1996).
[12] M. Maurer *et al.,* Europhys. Lett. **9**, 803 (1989).
[13] M. Albrecht *et al.,* Surf. Sci. **397**, 354 (1998).
[14] M. Albrecht *et al.,* Surf. Sci. **415**, 170 (1998).
[15] Z. Nishiyama, Sci. Rept. Tohoku Univ. **23**, 638 (1934); G. Wassermann, Arch. Eisenhuttermn. **16**, 647 (1933).
[16] E. Fullerton *et al.,* Phys. Rev. B **45**, 9292 (1992).
[17] C. Brouder, J. Phys. Condens. Matter **2**, 701 (1990).
[18] P. Le Fevre *et al.,* Phys. Rev. B **52**, 11 462 (1995).
[19] P. A. Lee *et al.,* Rev. Mod. Phys. **53**, 769 (1981).
[20] W. L. O'Brien *et al.,* J. Appl. Phys. **76**, 6462 (1994).
[21] D. Arvanitis *et al.,* in *Spin-Orbit Influenced Spectroscopies of Magnetic Solids,* edited by H. Ebert and G. Schütz (Springer-Verlag, Berlin, 1996).